DEVELOPMENTAL BIOLOGY **173,** 228–242 (1996)
Article No. 0019

Cell Autonomous Expression of Perlecan and Plasticity of Cell Shape in Embryonic Muscle

Donald G. Moerman,*,†,[1] Harald Hutter,* Gregory P. Mullen,† and Ralf Schnabel*

**Max-Planck-Institut Für Biochemie, D-82152 Martinsried, Federal Republic of Germany; and †Department of Zoology, University of British Columbia, Vancouver, British Columbia, Canada V6T 1Z4*

Perlecan, a component of the extracellular matrix (ECM), is essential for myofilament formation and muscle attachment in *Caenorhabditis elegans*. We show here that perlecan is a product of muscle and that it behaves in a cell autonomous fashion. That is, perlecan expressed in an individual muscle cell does not spread beyond the borders of the ECM underlying that cell. Using a polyclonal antibody that recognizes all isoforms of perlecan, we demonstrate that this protein first appears extracellularly at the comma stage (approx. 350 min) of development. We also show that during morphogenesis muscle cells have a heretofore undescribed plasticity of shape. This ability to regulate cell shape allows cells within a muscle quadrant to compensate for missing cells and to form a functional quadrant. A dramatic example of this morphological flexibility can be observed in animals in which the D blastomere has been removed by laser ablation. Such animals, lacking 20 of the 81 embryonic body wall muscle cells, can survive to become viable adult animals indistinguishable from wildtype animals. This demonstrates that the assembly of an embryo via a stereotypic lineage does not preclude a more general regulation during morphogenesis. It appears that embryos are flexible enough to immediately compensate for drastic alterations in tissue composition, a feature of development that may be of general importance during evolution.

INTRODUCTION

How cells interact to form a functional unit during morphogenesis is not well understood. The study of muscle development in the nematode *Caenorhabditis elegans* offers an experimental approach to exploring parameters necessary to form such a unit. Body wall muscle in the nematode *Caenorhabditis elegans* arises from four of the six early founder cells established after the first three rounds of cell division (Sulston *et al.*, 1983). These blastomeres, named AB, MS, C, and D, give rise to 1, 28, 32, and 20 muscle cells, respectively. Only the D blastomere gives rise to muscle cells exclusively (Fig. 1). Each of the other blastomeres give rise to nonmuscle cell types in addition to muscle. Most of the presumptive body wall muscle cells are born between 240 and 320 min post-first cell division (Sulston *et al.*, 1983). At about 290 min many of these muscle cells can be observed adjacent to the lateral hypodermal seam cells (Sulston *et al.*, 1983). Over the next hour these cells will migrate, either dorsally or ventrally, some will divide once more, and eventually all 81 cells will come to rest adjacent to the dorsal or ventral hypodermis, where they will form the four body wall muscle quadrants (Fig. 1). Each muscle quadrant is two cells wide and extends the length of the animal. Unlike vertebrate muscle, nematode body wall muscle cells do not fuse to form a multinucleate myotube. Instead, these mononucleate cells adhere tightly to adjacent muscle cells within a quadrant as well as to the underlying extracellular matrix and hypodermis (Waterston, 1988; White *et al.*, 1986; Francis and Waterston, 1985, 1991). This arrangement allows for coordinated contraction and relaxation within a muscle quadrant and for the direct transmission of contractile force to the cuticle of the animal.

[1] To whom correspondence should be addressed. Fax: (604) 822-2416. E-mail: moerman@bcu.ubc.ca.

0012-1606/96 $12.00

The interplay between muscle and hypodermis during growth and development of the nematode is coming under intense scrutiny as we try to understand the events that lead to the morphogenesis of muscle (Francis and Waterston, 1991; Goh and Bogaert, 1991; Hresko *et al.*, 1994). The importance of the hypodermis for late morphogenetic events, particularly elongation of the embryo, has long been recognized (Sulston *et al.*, 1983; Priess and Hirsh, 1986), and the necessity for intact functional muscle to facilitate this elongation is now well documented (Waterston, 1989; Barstead and Waterston, 1991; Williams and Waterston, 1994). Communication between hypodermis and muscle occurs through the basement membrane, a thin, 20-nm-thick sheet of extracellular matrix (ECM) (White, 1988). Genetic analysis of the ECM shows that it too is important in late embryogenesis, specifically for muscle formation (reviewed in Kramer, 1994). For example, mutations in type IV collagen or perlecan or overexpression of SPARC/osteonectin all lead to alterations in muscle during embryogenesis and thus to a lethal phenotype (Guo *et al.*, 1991; Sibley *et al.*, 1993; Rogalski *et al.*, 1993; Schwarzbauer and Spencer, 1993).

The *unc-52* gene of *C. elegans* encodes a protein homologous to the major mammalian basement membrane proteoglycan, perlecan (Rogalski *et al.*, 1993). Genetic studies of *unc-52* mutants in *C. elegans* demonstrate that this protein has a role in muscle attachment late in development (Brenner, 1974; MacKenzie *et al.*, 1978; Waterston *et al.*, 1980) and in sarcomere organization and anchorage during late embryogenesis (Rogalski *et al.*, 1993; Williams and Waterston, 1994; Hresko *et al.*, 1994). In this study we use a polyclonal antibody that recognizes all isoforms of UNC-52 (perlecan) to determine how early during development and in what tissues this protein is expressed. During embryogenesis we find that perlecan is made exclusively in muscle. Perlecan is not detectable within the ECM until just before it is functionally required for sarcomere organization and attachment of the muscle cell. We also show that perlecan, although a component of the ECM, behaves as a cell autonomous product of muscle. It does not diffuse, nor is it transported to regions underlying adjacent cells. These observations, coupled with the previous phenotypic characterization of a null mutant (Williams and Waterston, 1994; Hresko *et al.*, 1994; Rogalski *et al.*, 1993, 1995), lead us to conclude that the primary function of perlecan is anchoring the myofilament lattice and that perlecan has no role in muscle cell migration.

While investigating the cell autonomous behaviour of perlecan, we discovered that developing muscle cells could compensate for missing cells and reestablish a continuous muscle quadrant. Such muscle quadrants lack as many as 6 of the normal contingent of 21 cells (Fig. 1), yet in many instances they are functional. This plasticity of cell shape and ability to compensate for missing muscle cells has not previously been observed during *C. elegans* embryogenesis and points to another level of regulation during the morphogenetic phase of this process. We suspect this plasticity of form reflects the underlying cooperativity that must exist between interacting muscle cells and between muscle cells and the hypodermis in building a functional muscle quadrant.

MATERIALS AND METHODS

Strains and culture conditions. The wildtype Bristol N2 strain was used for all experiments (Brenner, 1974). Strains were grown on NG agar plates as described by Brenner (1974).

Microscopy, laser ablations, and immunostaining procedures. All microscopy was done using either Zeiss Axiophot or Axioplan microscopes equipped with DIC and epifluorescence optics. A VSL-337ND dye laser (wavelength 450 nm, Laser Science Inc.) at a setting of 20 laser pulses per second was used for all blastomere laser ablations (Hutter and Schnabel, 1994). Depending on the calibration of the laser, blastomeres were irradiated anywhere from 30 to 90 sec. All ablations were performed at 25°C. During irradiation blastomeres were monitored and continuous pulses were administered until we observed increased motion of yolk granules and the start of nuclear breakdown. At times, blebbing of the blastomere was observed and occasionally irradiated blastomeres divided once. Surrounding blastomeres were also monitored for laser-induced damage and in cases in which this was observed these animals were discarded.

In the experiments in which ablated embryos were eventually to be stained for immunofluorescence, eggs were mounted in a drop of water on a poly-lysine-coated multiwell slide. Teflon-coated multiwell slides with more than a 20-μm clearance (H. Hölzel, Dorfen, FRG) allow for normal development and constrain the embryo between slide and coverslip. Ablated animals were incubated at 25°C until they reached the 1.5- to 2-fold stage of development (approximately 4 to 5 hr postablation). A freeze-fracture method was used to prepare embryos for immunofluorescence. Slides were frozen on dry ice and the coverslip was removed with a razor blade. Samples were then fixed in cold (−20°C) methanol for 5 min, postfixed in cold (−20°C) acetone for 5 min, and then incubated at room temperature in 0.5% Tween 20/PBS (0.1 *M* sodium phosphate, pH 7.0, 0.1 m*M* EDTA) for 5 min. Slides were then gently dried so as not to disturb the well with ablated embryos and then primary sera was added to the well. For most experiments we used the rabbit polyclonal sera GM1 (see below) to monitor perlecan distribution, together with a monoclonal antibody, either NE8 4C6.3 (Goh and Bogaert, 1991) or DM5.6 (Miller *et al.*, 1983), to monitor muscle integrity. Slides with primary antibodies were then incubated in a ''humidity chamber'' (petri dish with damp paper) at 4°C overnight. These samples were next transferred to a Coplin jar with Tween 20/PBS for 5 min. After this the slides were again

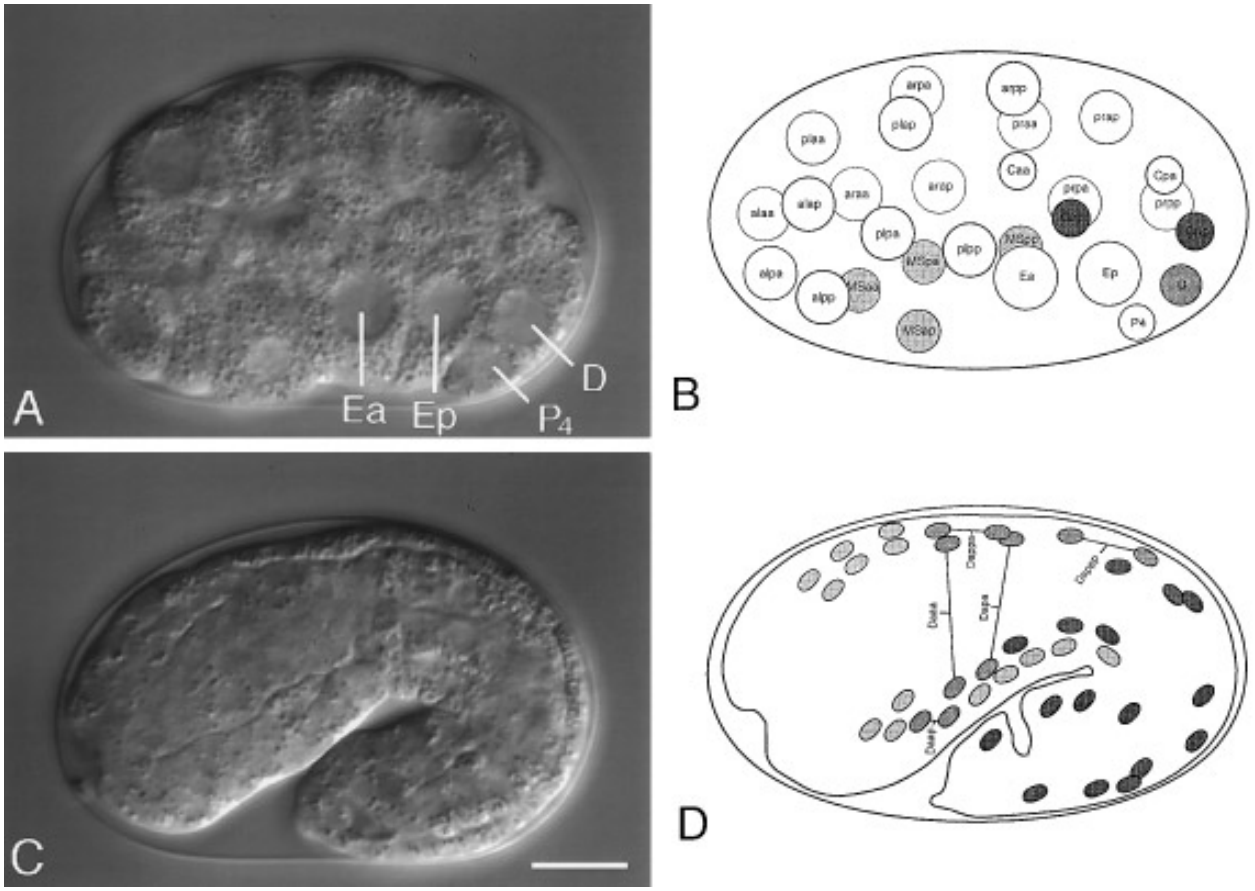

FIG. 1. Position of D blastomere and D-derived muscle cells. Anterior is to the left. (A and C) are left lateral midplane views of the developing embryo using Nomarski optics. (A) An embryo at the beginning of gastrulation (approx. 100 min). The intestinal precursors, Ea and Ep, are useful landmarks at this stage. The germline precursor, P4, is the sib of D. (B) A drawing showing the position of all 28 nuclei at the stage illustrated in (A). The six muscle precursors are shaded. (C) A view of a 1.75-fold embryo (430 min) when the first movements are detected. The outline of the pharynx can be seen. (D) A drawing of the stage shown in (C) with the relative positions of the 40 body wall muscle nuclei on the left side of the embryo illustrated (modified from Sulston *et al.*, 1983). Note that Da contributes cells to both the left dorsal and ventral quadrants. Also note that the six dorsal cells form a central patch of muscle in the dorsal quadrant. All time points denoted here and in subsequent figures are estimates based on Sulston *et al.* (1983). Bar, 10 μm.

dried gently and secondary antibodies were added. To detect GM1 we used TRSC-labeled affinity-purified goat anti-rabbit IgG, while to detect the mouse monoclonals we used FITC-labeled affinity-purifed goat anti-mouse IgG (Jackson ImmunoReseach Lab., Inc.). Secondary antibodies were diluted from 1:50 to 1:200 before being used. Samples were incubated with secondary antibodies for at least 2 hr at 20°C. Slides were then placed in Tween 20/PBS for 5 min and again dried gently. Finally, samples were mounted for observation using a mounting medium of 2.5% DABCO, 90% glycerol, and TBS, pH 8.5.

Time-lapse recording, lineage analysis, and rescue of ablated animals. Time-lapse recordings of embryos were done using a 4-D microscope (Hird and White, 1993; Hutter and Schnabel, 1994). Embryos were mounted in a drop of water on an agar pad under a coverslip and this was sealed with grease (procedure of Sulston *et al.*, 1983). In experiments in which we wanted to follow the D lineage in wild-type embryos or the C and MS lineages in ablated embryos, a series of 25 focal levels through the embryo were recorded every 30 sec for 5–6 hr at 25°C. In ablated embryos in which we wished to observe the period of elongation between two- and threefold, a recording was made every minute after 7 hr. For lineage analysis, the recordings were played in time-lapse mode and the behavior of individual cells was followed on a monitor. This aspect of our analysis relied on a modified version of John White's lineaging program (Hutter and Schnabel, unpublished research). To rescue D ablated animals that hatched, we first removed the grease from around the coverslip and then added a drop of water to the

edge of the coverslip. This slightly relieved the pressure on the animals and usually allowed us to slide the coverslip off the agar pad without removing or damaging the L1 animals. These were then transferred in a drop of water using a microcapillary to a bacteria-seeded plate to grow.

Construction of pGEX–unc-52 fusion and generation of the GM1 antisera. A 260-bp *Bam*HI/*Eco*RI fragment from plasmid DM #180 (Rogalski *et al.*, 1993) was gel purified and cloned into pGEX-2T (Smith and Johnson, 1988). A positive clone, DM #184, was identified using the mass screening method of Smith and Johnson (1988) and verified by restriction enzyme digestion of the plasmid DNA. Large-scale growth and purification of the fusion protein was as described (Smith and Johnson, 1988). To generate rabbit polyclonal antibodies, approximately 1.0 mg of purified fusion protein was emulsified in Freund's complete adjuvant and injected subcutaneously into two New Zealand White rabbits (0.5 mg each). Rabbits were boosted at 4-week intervals with 0.25 mg fusion protein emulsified in Freund's incomplete adjuvant and blood samples were taken 10 to 12 days postinjection. The immune response was monitored by using Western blots of purified fusion and carrier (GST) and by immunofluorescent staining of *C. elegans* embryos. Western blots were performed using the method of Towbin *et al.* (1979) as described in Rogalski *et al.* (1993). For immunofluorescent staining of embryos, staining with the preimmune sera, as well as staining of an *unc-52* null allele (Rogalski *et al.*, 1993, 1995) were used as controls for nonspecific staining. Immunofluorescence techniques used in this section were as described in Rogalski *et al.* (1993).

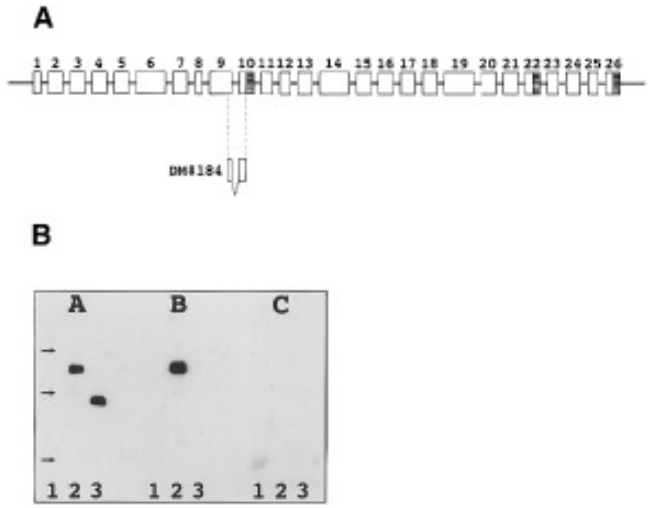

FIG. 2. Western blot demonstrating reactivity of the GM1 sera. (A) A schematic illustrating the exon structure of the *unc-52* gene. There are 26 exons in total and the hatched regions indicate alternative poly(A) addition sites (see Rogalski *et al.*, 1993 for details). The plasmid DM #184 is a pGEX plasmid containing the portion of exons 9 and 10 shown. A fragment containing these exons was subcloned from a cDNA that extended through this region. (B) A Western blot hybdridized in (A) with an antibody to GST (1:2000 dilution), in (B) with the GM1 sera (absorbed against GST and used at a 1:20,000 dilution), and in (C) with the preimmune sera (1:1000 dilution). Lane 1 in each case contains the molecular weight markers. From top to bottom, the three arrows indicate 45, 29, and 18 kDa, respectively. Lane 2 in each case is the GST–perlecan fusion expressed by plasmid DM #184. Lane 3 in each case is the GST polypeptide expressed by the pGEX vector. (A) We show that an antibody to GST recognzes GST (lane 3) and a larger fusion protein (lane 2). (B, lane 2) This larger fusion protein is also recognized by the GM1 sera. The GM1 sera after being preabsorbed to GST is specific for the perlecan portion of the fusion polypeptide (compare B, lanes 2 and 3). (C) This demonstrates that there is no reactivity to either GST or perlecan in the preimmune sera.

RESULTS

Perlecan, the ECM Proteoglycan Underlying Muscle Quadrants, Is Exclusively Derived from Body Wall Muscle Cells during Late Embryogenesis

Perlecan as a component of the ECM underlying muscle could be made and exported by either muscle or hypodermis. Earlier studies suggested that perlecan is a product of muscle (Francis and Waterston, 1991; Hresko *et al.*, 1994; Rogalski *et al.*, 1995; see discussion for details). However, because the *unc-52* gene which encodes perlecan can generate a number of isoforms of the protein via alternative splicing (Rogalski *et al.*, 1993, 1995), it is possible that these studies missed the expression of other isoforms of this protein. The monoclonal antibody used in previous studies, MH2/3, does not detect all isoforms of this protein (G.M. and D.G.M., unpublished results and see below). To determine if perlecan isoforms are made by the hypodermis as well as by muscle and to determine the earliest occurrence of a perlecan isoform, we have done immunofluorescence studies of embryos using a new antibody that recognizes all isoforms of perlecan. To stage embryos we have used the monoclonal antibody MH27, which recognizes hypodermal cell boundaries (Francis and Waterston, 1991). The position and shape of these cells act as convenient markers for late stages in embryonic development (Sulston *et al.*, 1983; Goh and Bogaert, 1991; Hresko *et al.*, 1994; Podbilewicz and White, 1994). To identify body wall muscle cells and view the organization of the sarcomeres, we used the monoclonal antibody DM5.6, which specifically recognizes the body wall muscle myosin heavy chain—myoA (Miller *et al.*, 1983). To ensure that we are detecting all isoforms of perlecan, we have generated a polyclonal serum reactive to a region of UNC-52 expressed in all variants of perlecan. The polyclonal serum, GM1, is directed to a region of UNC-52 encoded by a portion of exons 9 and 10 (see Fig. 2A). This region encodes part of the second laminin repeat of domain III of the gene (Rogalski *et al.*, 1993) and appears to be expressed in all UNC-52 variants (Rogalski *et al.*, 1995; G.M.

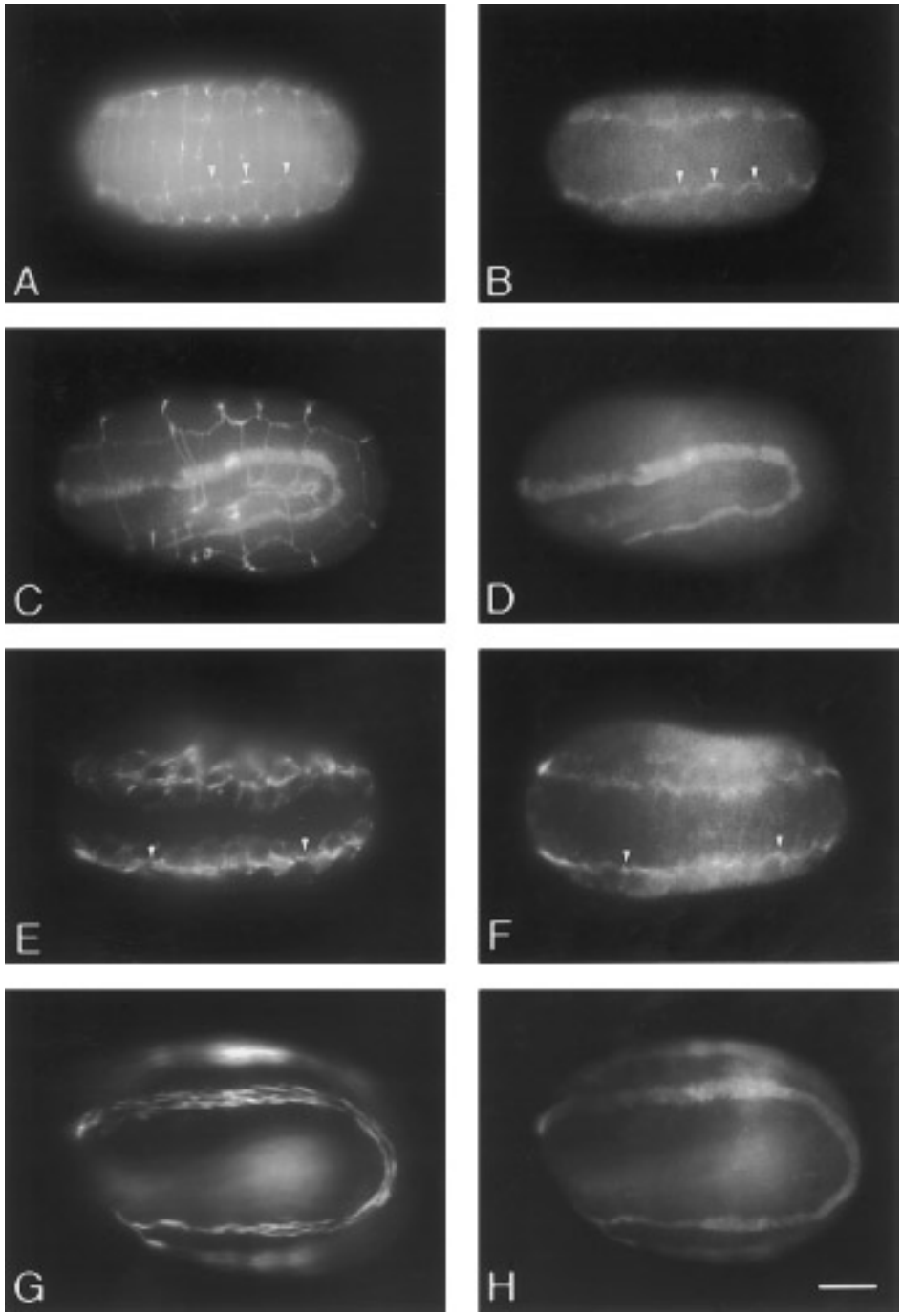

FIG. 3. Fluorescence micrographs illustrating the time of expression of perlecan within a *C. elegans* embryo. Anterior is to the left in all micrographs. (A and B) A dorsal view of an early comma stage embryo (approx. 350 to 390 min). Both dorsal muscle quadrants are visible. (A) MH2/3 and MH27 staining; (B) GM1 staining. The grid-like pattern of MH27 outlines the hypodermal cells in (A). MH2/3 and GM1 staining is coextensive. Arrowheads in (A) and (B) identify identical regions. (C and D) A left ventral–lateral view of a 1.75-fold embryo (approx. 430 min) and focuses on the left ventral muscle quadrant. (C) MH2/3 and MH27 staining; (D) GM1 staining. Again, the grid-like pattern of MH27 outlines the hypodermal cells in (C). As in the earlier stage, MH2/3 and GM1 staining are coextensive. (E and F) A dorsal view of an early comma stage embryo (approx. 350 to 390 min) with both dorsal muscle quadrants visible. (E) DM5.6 staining of myosin; (F) GM1 staining of perlecan. Myosin staining in (E) is distributed over the entire muscle cell, but is concentrated in regions where muscle cells contact each other and the underlying hypodermis. Hresko *et al.* (1994) refer to this as muscle cell polarization. (F)

and D.G.M., unpublished results). The serum is reactive on a Western blot to the original GST–UNC-52 fusion protein used to generate the serum (Fig. 2B). To ensure that the serum is specific to protein products of *unc-52,* we have stained a null allele of the locus, *st549* (Rogalski *et al.,* 1995) and find no detectable staining either of the basement membrane underlying body wall muscle or of any other tissue (data not shown).

In comma stage embryos GM1 reacts with the basement membrane underlying body wall muscle and has a similar distribution to MH2/3 (Figs. 3A and 3B). In twofold embryos GM1 and MH2/3 stain the basement membrane underlying muscle quadrants in a similar manner (Figs. 3C and 3D), but at this stage GM1 also stains the presumptive pharynx (data not shown). MH2/MH3 staining of the pharynx is not detectable until much later in development. Therefore, isoforms not recognized by MH2/3 are present during embryogenesis, but like MH2/3 recognized isoforms, these appear to be expressed only by muscle. In an early comma stage embryo myosin is found throughout the cytoplasm of a muscle cell, but is concentrated in regions where muscle cells contact each other and the underlying hypodermis (Fig. 3E; also see Hresko *et al.,* 1994). A comparison of perlecan and myosin distribution in these embryos shows that perlecan is concentrated to regions of contact between adjacent muscle cells just under the regions of concentrated myosin (Fig. 3F). Faint staining of perlecan at the periphery of several muscle cells can also be observed at this stage (Fig. 3F), which again implies that the muscle cells are the primary source of perlecan. By the twofold stage of development, muscle sarcomeres are fully formed and discrete A-bands can be observed (Fig. 3G), and at this stage perlecan is localized to the basement membrane underlying the entire muscle quadrant (Fig. 3H).

The GM1 serum identifies additional perlecan isoforms not detected with MH2/3, but these additional isoforms are not expressed in tissues other than muscle during embryogenesis. In fact, the pattern we observe in a comma stage embryo using GM1 is very similar to that obtained using MH3 (see Hresko *et al.,* 1994). While structural components of muscle are detected as early as the 290-min stage of development (Epstein *et al.,* 1993; Hresko *et al.,* 1994), our attempts to identify perlecan expression earlier than the 350-min stage with either GM1 or MH2/3 were inconclusive. A patchy staining of perlecan associated with muscle was sometimes observed in earlier embryos (G.M., H.H., and D.G.M., unpublished results).

Perlecan Is a Cell Autonomous Product of Muscle

The discovery that muscle is the only source of extracellular perlecan led us to question how perlecan is distributed extracellularly. The following experiment was done to determine whether secreted perlecan remains locally or moves away from the muscle cell of origin, by either diffusion or active transport. The experiment takes advantage of the defined lineage of *C. elegans* (Sulston *et al.,* 1983). Using a laser, one can ablate specific precursors and determine the consequences of this operation later in development. We used a laser to remove either the D blastomere or one of its daughters, Da or Dp. The D blastomere behaves in a strictly mosaic manner; i.e., the removal of D leads to the loss of cells derived from that precursor (Sulston *et al.,* 1983; Junkersdorf and Schierenberg, 1992). The D blastomere gives rise to 20 of the 81 embryonic body wall muscle cells. These 20 cells are distributed to all four muscle quadrants, 6 cells to each dorsal quadrant and 4 to each ventral quadrant (Sulston *et al.,* 1993; Fig. 1). D-derived body wall muscle cells located in the dorsal quadrants are found in the middle region of a twofold embryo. The daughters of D, Da and Dp, each give rise to 10 cells. Da gives rise to body wall muscle cells of the left dorsal and ventral quadrants (Fig. 1D), while Dp gives rise to cells of the right dorsal and ventral quadrants.

We ablated D, Da, or Dp and double-labeled the ablated embryos with a monoclonal antibody specific to muscle thick filaments to identify muscle cells and the polyclonal sera, GM1, to detect perlecan. Similar to earlier observations (Sulston *et al.,* 1983), we observed a gap between anterior and posterior muscles in the dorsal quadrants at the position where D-derived muscle cells should be located in late embryos (Table 1 and Figs. 4C, 4F, and 4I; but see below). In all cases the ECM component perlecan colocalized with the underlying muscle (Figs. 4B and 4E). Examples of Da-, Dp-, and D-ablated animals are shown (Fig. 4). The results with all three types of ablations are consistent—muscle and perlecan staining are coextensive. These results demonstrate that a muscle-derived ECM component behaves in a cell autonomous fashion. That is, perlecan is only found adjacent to the cell that actively expresses it.

Plasticity of Muscle Cell Shape during Morphogenesis

Several ablations of D, or D(a/p), blastomeres led to animals with no apparent gaps in either the dorsal or the ven-

Perlecan staining appears concentrated to regions of contact between adjacent muscle cells. The arrowheads in (E) and (F) point to identical spots and show that the regions of concentration of myosin are directly under the regions of concentration of perlecan. Note also a faint staining of perlecan at the periphery of several muscle cells in (F). (G and H) The left dorsal muscle quadrant of a twofold embryo (approx. 450 min). (G) DM5.6 staining of myosin; (H) GM1 staining of perlecan. Muscle sarcomeres are fully formed at this stage and in (G) one can discern discrete A-bands (two per cell at this stage). Also at this stage, perlecan (H) is localized to the basement membrane underlying the entire muscle quadrant. Bar, 10 μm.

TABLE 1
Muscle Blastomere Ablations and Muscle Cell Plasticity

	Da	Dp	D[a]	Total[b]
Observable gap in dorsal quadrant	4 (1)[c]	8 (2)	7 (6)	19
No gap in dorsal quadrant	2 (1)	3 (3)	9 (4)	14

[a] Of seven D ablated embryos with gaps, five had both dorsal quadrants visible. Only two of the five had gaps in both dorsal quadrants.

[b] A total of 104 blastomere laser ablation operations were attempted. Embryos were lost due to a number of causes, including killing the embryo by damaging adjacent blastomeres to D, losing embryos from slides during fixation or staining, poor immunostaining, or inappropriate orientation of embryo for evaluation of muscle quadrant.

[c] Number in parenthesis is the number of embryos with identifiable excluded material. Number not in parenthesis is the sum of animals with excluded ablated material together with animals having included ablated material.

tral muscle quadrants. As shown in Table 1, ''gap repair'' occurred quite often. Table 1 shows only the data for the dorsal quadrants and includes only those embryos in which we were able to positively identify the ablated material. In all of these embryos at least one ventral quadrant was examined but no gaps were detected. Gap repair of dorsal muscle quadrants was independent of whether the ablated material was excluded from the embryo or retained within the embryo. Figure 5 illustrates this phenomenon of gap repair. In this example D was ablated, yet both dorsal quadrants have continuous muscle (Figs. 5B and 5C), and perlecan is continuous within the ECM (Figs. 5E and 5F). Note that in each dorsal quadrant 6 of 21 muscle cells are missing. Examples of ventral quadrant gap repair are shown in Figs. 4B, 4C, and 4H. This flexibility for muscle at the morphological level stands in marked contrast to the more restrictive deterministic developmental program for muscle in *C. elegans.* This ability of cells to compensate for missing components and to establish a functional structure, in this case a continuous muscle quadrant, we will refer to as ''plasticity'' of form. Sulston and White (1980) have observed a similar phenomenon postembryonically. Our observations demonstrate that cellular plasticity can occur during embryonic development as well.

It is muscle cells derived from the C and MS blastomeres that compensate for the missing D-derived cells. These muscle cells appear to do so by elongating their processes and/or by migrating into the region. A comparison of the distribution of muscle cells and their processes in an unablated embryo and an ablated embryo (Figs. 5A and 5B, respectively) suggests that both possibilities may contribute to gap filling. The spacing of cell nuclei in the ablated region of a dorsal quadrant appears altered, suggesting that there has been some migration into the region. However, these cells also appear more extended than a typical cell for this region of the embryo.

In order to understand the dynamics of how muscle repair might occur in the ablated embryos we have examined wildtype embryos fixed and stained with a muscle marker (Fig. 6) and compared these to muscle cell migrations followed using the 4-D microscope and the lineaging program. The first presumptive muscle cells are born at approx. 240 min post-first cleavage and the last are born at about 350 min (Sulston *et al.*, 1983). The process of muscle migration from a position adjacent to the seam cells to one adjacent to the dorsal, or ventral, hypodermal cells commences at approx. the 290-min stage and extends to the 350-min stage (Sulston *et al.*, 1983; Hresko *et al.*, 1994). Thus cell division is still occurring while cells are migrating into their final positions to form a muscle quadrant. For example, some of the last muscle cells born are the dorsal progeny of D(a,p)ppa and D(a,p)ppp. The more anterior of these sibs divides while migrating toward the dorsal surface, while the latter does not divide until after intercalating into the quadrant (Sulston *et al.*, 1983; our observations).

At 290 min the muscle cells are in four rows along the side of the animal. By the 310-min period a small space has opened up between the dorsal and the ventral double rows of cells in the anterior portion of the embryo (Fig. 6A; also see Epstein *et al.*, 1993). Note that in the posterior portion of the embryo the muscle cells still form a continuous sheet of cells. By the 330-min period the space between the dorsal and the ventral cells has widened and has also extended further posterior in the embryo (Fig. 6B). Spaces have also opened between C-derived putative dorsal and ventral muscle cells. By 350 min most muscle cells have joined their appropriate quadrant (Fig. 6C), and by 420 min they have flattened against the underlying basement membrane and hypodermis (Fig. 6D; also see Hresko *et al.*, 1994). A gap between muscle cells as a consequence of ablating the D blastomere can be observed quite early during this migration process. Figure 4I shows an embryo at approx. 310 to 330 min and a gap is clearly visible. Between the migration of cells and their further division there is certainly opportunity for cells that normally may not touch each other to come into contact. It is also clear that muscle processes could span such a gap once in contact. Processes bridging the interval between cells of the dorsal and the ventral quadrants can be seen to persist for some time (see Fig. 6C, for example).

The D Blastomere Is Not Essential for Viability

Our observation that removal of the D blastomere could lead to a twofold embryo with intact dorsal muscle quadrants and wildtype appearance led us to speculate on how far such an animal would develop. Would such an animal elongate properly to a threefold worm and would it be capable of hatching? If it hatched, would it grow and how would it move? Would it be uncoordinated? To address these ques-

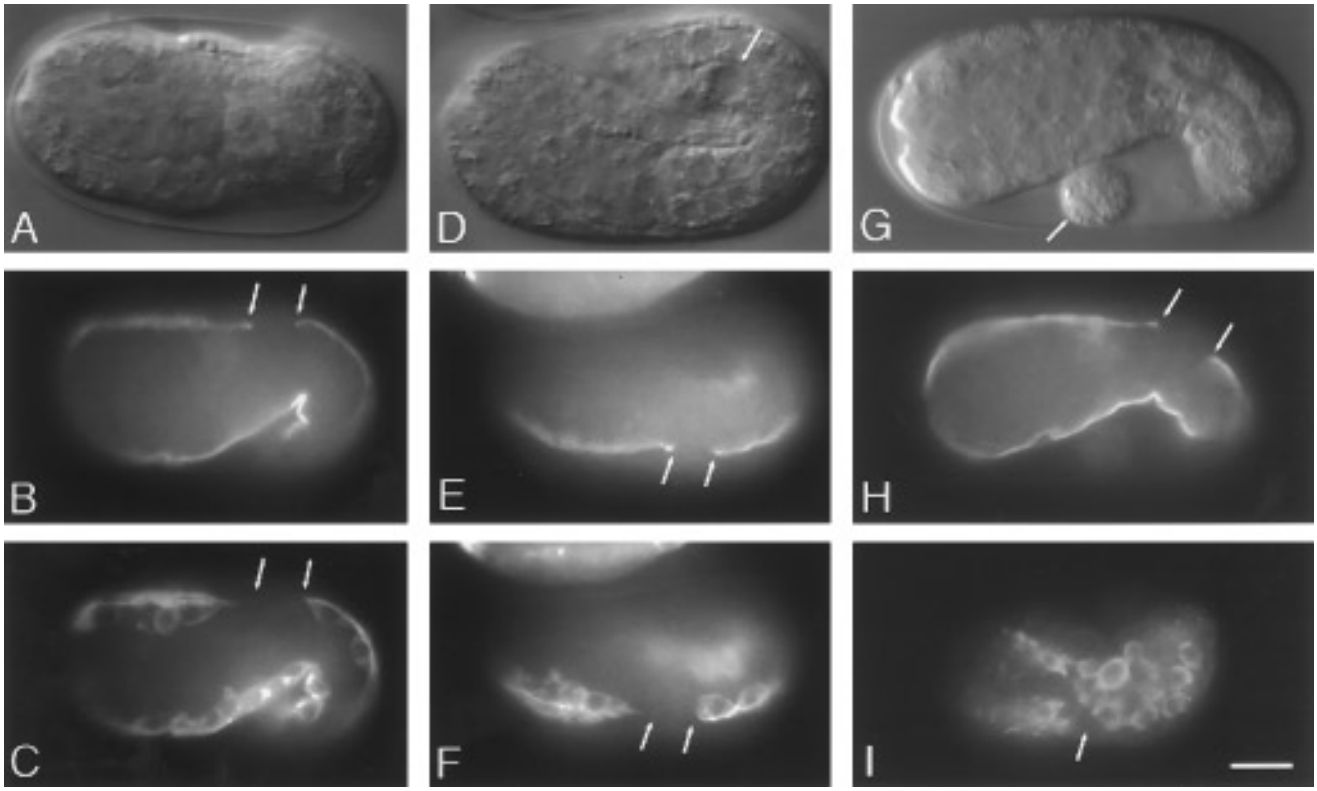

FIG. 4. Cell autonomous expression of myosin and perlecan in Da (A, B, and C)-, Dp (D, E, and F)-, and D (G, H, and I)-ablated embryos. Anterior is to the left for all of these embryos, which range from very early comma to almost twofold (330 to 450 min). (A) A Nomarski optics micrograph showing the Da-ablated material in a 1.5-fold embryo. Since Da gives rise to cells on the left side of the animal (see Fig. 1), the fluorescence micrographs (B) and (C) show a left lateral view of the dorsal and ventral body wall muscle quadrants. (B) is stained with GM1, which identifies perlecan. (C) is stained with NE8 4C6.3, which identifies a muscle thick filament component (D.G.M., personal observation). In (C) there is a gap in staining where the Da-derived muscle cells are located in the dorsal quadrant (arrows point to boundaries of the gap). This gap is bounded by MS- and Cap-derived muscle cells. In (B) perlecan staining is also discontinuous along the dorsal quadrant. The arrows in (B) identify the same region as the arrows in (C). Note that no gap is visible in the ventral muscle quadrant in either (B) or (C). (D) A Nomarski optics micrograph of a Dp-ablated embryo (arrow points to ablated material) in an almost twofold embryo. Since Dp gives rise to cells on the right side of the embryo, (E) and (F) show a view of the right dorsal body wall muscle quadrant. In (E), stained with GM1, there is a gap in perlecan staining underlying this dorsal muscle quadrant (see region identified by arrows). In (F), stained with NE8 4C6.3, there is again a gap in the dorsal muscle cell staining, where the Dp-derived muscles should be located (see area bounded by arrows). From the position of the arrows in (E) and (F), it is clear that these gaps are in equivalent postions. In both embryos perlecan (B and E) does not extend beyond the borders of a muscle cell (C and F). (G and H) A left lateral view of a D-ablated embryo at the late comma to 1.25-fold stage of development. The left dorsal and ventral muscle quadrants are both visible in this animal, which has developed to about the 400-min stage. (G) A Nomarski optics micrograph of the embryo that shows the D-ablated material outside of the embryo (arrow). (H) A fluorescence micrograph of the same embryo stained with GM1. Arrows mark the discontinuous staining of the left dorsal quadrant. Again, note that as in (B) the ventral quadrant does not have a gap in staining. In this animal the dorsal right quadrant did not show a gap (data not shown). (I) A D-ablated embryo at early comma stage (approx. 330-min post-first cleavage) stained with NE8 4C6.3. In this embryo anterior is to the left and dorsal is on the bottom. This is a right lateral view of the embryo and muscle cells are in the process of migrating from lateral positions next to the seam cells to positions adjacent to the dorsal and ventral hypodermal cells. A gap is clearly visible between cells migrating toward the dorsal quadrant. (Compare this panel to Figs. 6A and 6B). Bar, 10 μm.

tions we did a second series of D blastomere ablations, but this time we maintained the animals after the operation to observe their growth and behavior.

Of 70 D blastomere-ablated embryos, 32 eventually reached the threefold/hatching stage. The death of several D-ablated embryos during embryonic development was probably not due to the loss of the D blastomere or its descendants per se. Of 70 ablated embryos, 6 died shortly after D was ablated (usually within one division round). In all of these cases we noted damage to blastomeres in addi-

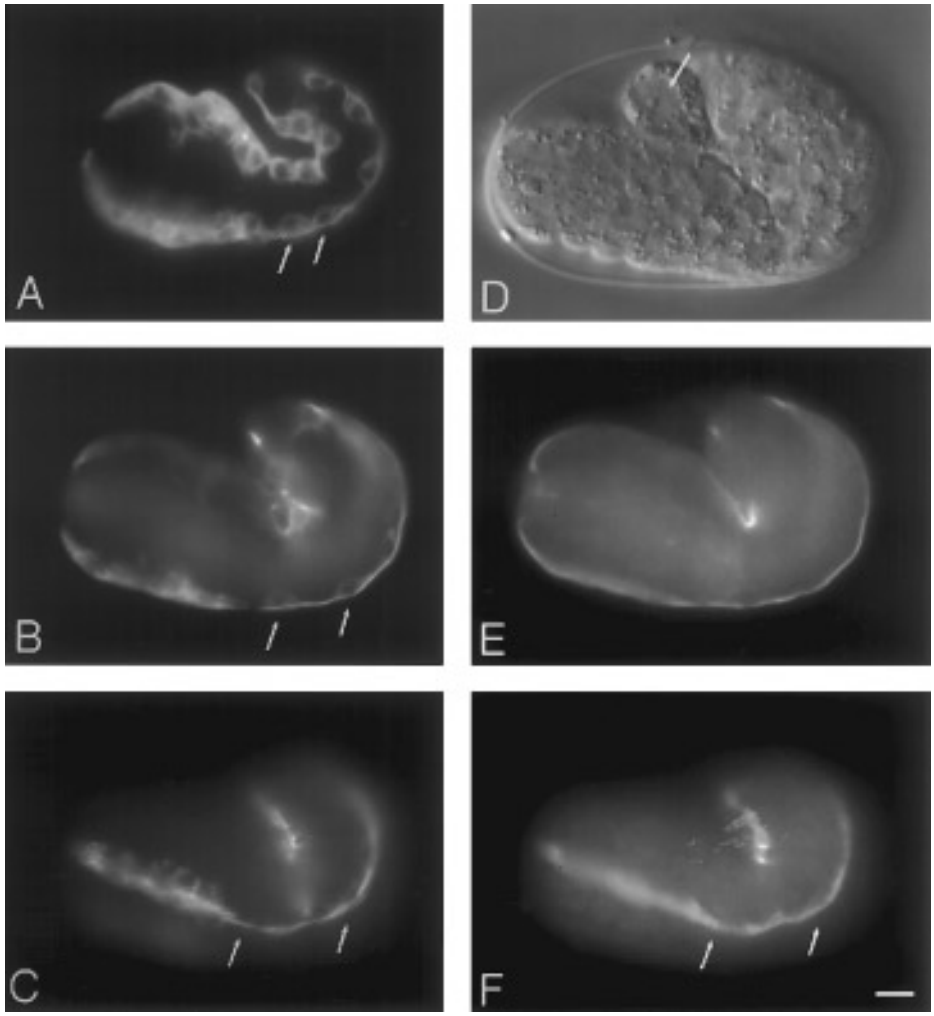

FIG. 5. Muscle plasticity in a D blastomere-ablated embryo. (A) A fluorescence micrograph of a wildtype unablated 1.5-fold embryo (approx. 420 min) stained with NE8 4C6.3. Anterior is to the left and dorsal is down. A ventral and a dorsal muscle quadrant are visible in this embryo. Arrows point to two dorsal muscle cells to illustrate spacing in this region of the embryo at this stage. (B through F) Micrographs of a single D-ablated embryo. Again, this is a 1.5-fold stage embryo with anterior to the left and dorsal down. The animal is slightly turned, which gives a dorsolateral view. (D) A Nomarski micrograph illustrating the ablated material (arrow). (B and E) The left dorsal muscle quadrant stained with NE8 4C6.3 and GM1, respectively. (C) The right dorsal muscle quadrant stained with the muscle-specific antibody NE8 4C6.3; (F) the same quadrant stained with GM1. Arrows in (C) and (F) point out the region where a gap would be expected. No break in muscle staining is evident in either (B) or (C). Similarly, perlecan appears as a continuous band underlying the muscle of both dorsal quadrants (E and F). There is some difference in the spacing of dorsal muscle cells in these ablated animals, as shown in (B). Arrows point to a region with a different spacing of cells compared to (A) (compare arrows in A and B). Bar, 5 μm.

tion to D during laser ablation, or shortly after, due to over-ablation. Of 64 embryos that survived to the comma/two-fold stage of development, 32 continued to develop to the threefold/hatching stage. Those that hatched had one of two general phenotypes: they either were near normal in appearance (Figs. 7B and 7D), or were lumpy and had cuticular constrictions (Figs. 7F and 7H). These latter larvae were also severely uncoordinated and those similar in appearance to (H) usually did not develop much beyond the L1 larval stage. Whether the ball of ablated material was included or excluded from the embryo did not have a bearing on the L1 phenotype (see Figs. 7A–7H). From these data it is clear that an embryo can compensate for the lack of 20 body wall muscle cells. It can elongate, hatch, and even grow into an egg-laying adult (Table 2).

The observation that 32 of 64 ablated embryos died during the period of elongation from two- to threefold led us to consider whether this is a crucial period in morphogenesis

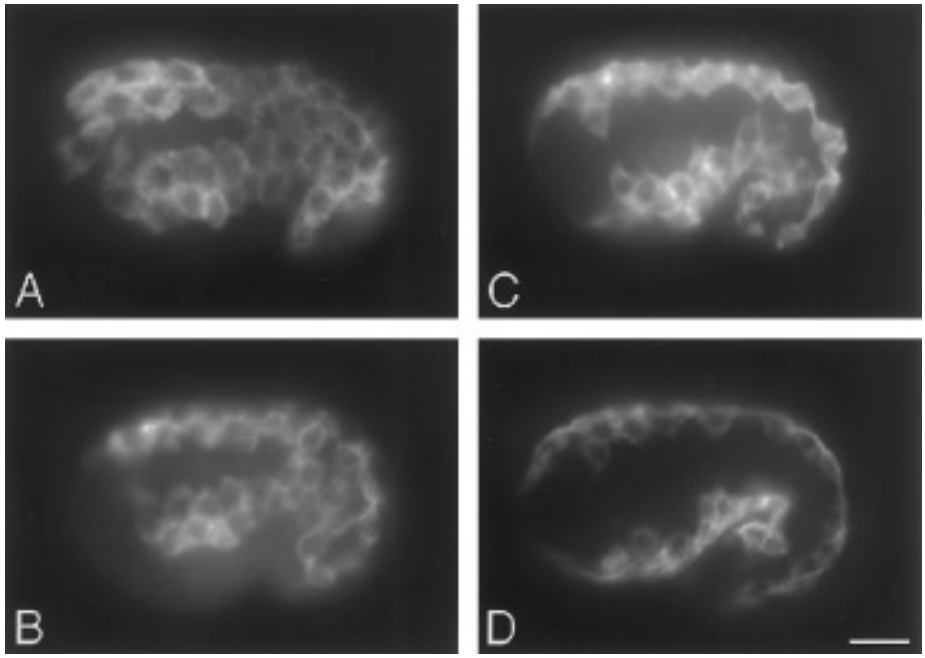

FIG. 6. Migration of muscle cells from a lateral position adjacent to seam cells to positions adjacent to dorsal and ventral hypodermal cells. These fluorescence micrographs show a left lateral view of embryos in which anterior is left and dorsal is at the top. The time period covers from early comma (A) to the 1.5-fold stage (D). Times are estimates based on Sulston *et al.* (1983), Epstein *et al.* (1993) and on direct comparison of these fixed and NE8 4C6.3-stained embryos to the 290- to 420-min interval of a recorded and analyzed lineage (our observations). (A) An embryo at approx. 310 min that shows cells in the anterior part of the embryo already separated and migrating away from the midline. Note that at this stage cells in the posterior half of the embryo form a continuous sheet of muscle cells. (B) An embryo at approx. 330 min that shows that more posterior muscle cells of the embryo are also now separated and migrating dorsally or ventrally. (C) An embryo at approx. 350 min; cells are now formed into dorsal and ventral muscle quadrants. (D) A 1.5-fold (420 min) embryo. The muscle cells are more flattened and myofilament formation is becoming apparent. Bar, 10 μm.

for such an individual. Closer examination of these individuals revealed that these deaths are only indirectly related to the ablation of the D blastomere. In the majority of these cases (28 of 30; no recording at this time period for two samples), the excluded D-derived material forms a continuity with the main body of the embryo. This attachment is illustrated in Fig. 7I, which shows the excluded material still attached to the main body of the embryo. Within 2 hr this embryo will turn into the ''monster'' shown in Fig. 7J. By contrast, note that panel C in this figure also has an embryo with an excluded ball, but in this example the ball is completely separate from the embryo. In this case a reasonable larva emerged (Fig. 7D). Embryonic death during elongation therefore appears to be a consequence of interference with closure of the embryo rather than a direct loss of muscle. As internal pressure within the embryo builds during elongation, cells will be pushed through this weak point (see Priess and Hirsh, 1986).

Fifteen of 32 animals that hatched were rescued and transferred to plates for further observation. Three of the 15 were similar in appearance to Fig. 7H and these animals died as young larvae. Eleven of the remaining 12 animals appeared near wild type as newly hatched L1 larvae and all were observed further to see if they would grow and if they were fertile. It is clear that an animal lacking 20 muscle cells can indeed reach egg-laying maturity (Table 2; only 1 of the remaining 12 animals died as a larva). As shown in Table 2, these individuals varied widely in phenotype but some were near wild type in appearance. Some of these individuals grew more slowly than wildtype animals, taking twice as long to reach egg-laying maturity. Many were also uncoordinated, or at least slower moving than wildtype animals. In at least two cases D-ablated animals did not reach the normal adult hermaphrodite length. These individuals were about two-thirds the length of a normal adult animal, even as fully mature animals. Brood size also varied a great deal between individuals. Four animals were sterile and four were semisterile (brood sizes < 40). Generally, brood size was a good indicator of the overall well-being of an animal. The four animals with the largest brood size also had the least impaired movement. The two animals with the largest brood size were virtually indistinguishable from wildtype animals.

The animals that appeared nearly normal in movement

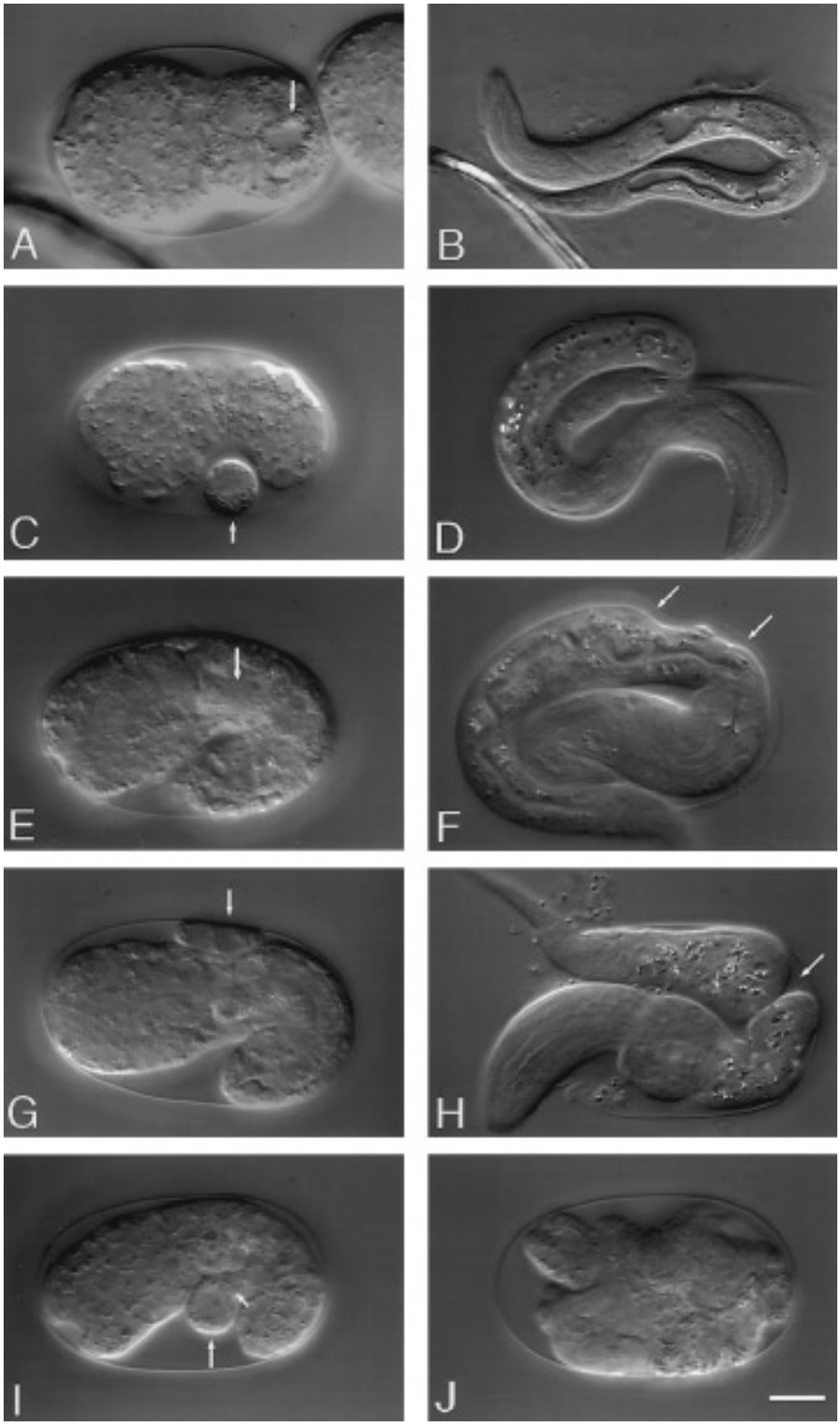

TABLE 2
Phenotypic Description of Animals Lacking a D Blastomere

Animals[a]	Survival to adult	Movement	Brood size
dm n2b 7.2[b]	Yes	Slow	0
dm n2b 10.1	Yes	Slow, unc	26
dm n2b 10.3	Yes	Very slow, unc	10
dm n2b 10.4	Yes	Wild type	266
dm n2b 10.5	Yes	Slow	32
dm n2b 11.4	Yes	Near wild type	121
dm n2b 12.2[c]	Yes	unc, paralyzed	13
dm n2b 13.5	Yes	Slow	0
dm n2b 13.6	No	—	—
dm n2b 14.3[b]	Yes	Wild type	198
dm n2b 15.1[b]	Yes	Near wild type	104
dm n2b scn1	No	—	—
dm n2b scn 2.1	Yes	Slow	0
dm n2b scn 2.2	No	—	—
dm n2b scn 2.3	No	—	—

[a] Each of these are individual D-ablated animals rescued after hatching.
[b] These three animals took at least twice as long to reach egg-laying maturity as rescued siblings that were not ablated. The other animals were not examined for this phenotype.
[c] This animal had noticeable constrictions as a newly hatched L1 larva.

and fertility demonstrate that the contribution of the D blastomere is not essential for viability and that the embryo has enough functional plasticity to compensate for the loss of one-quarter (20 of 81) of the embryonic muscle cells.

DISCUSSION

Perlecan is made in body wall muscle and is then transported out of muscle to the side adjacent to the underlying hypodermis. Francis and Waterston (1991) first suggested that perlecan might be made in muscle. In temperature-sensitive developmental arrest embryos, perlecan is detected only in myosin-producing cells, not in presumptive hypodermal cells (R. Francis and A. Curry, unpublished results). Embryos at comma stage accumulate perlecan in regions of contact between the muscle cells after the muscle cells have migrated from their lateral position under the seam cells to their final position under the dorsal hypodermal cells (Hresko *et al.*, 1994; this study). Over the next 2 hr (approx.) muscle sarcomeres will organize and become properly anchored, and the embryo will elongate to the two-fold stage. Based on the terminal phenotype of null alleles of *unc-52*, we conclude that this is the stage when perlecan function is first required (Rogalski *et al.*, 1983, 1995; Williams and Waterston, 1994). It is also the first time during morphogenesis when general body wall muscle function is required to aid in the elongation and shaping of an embryo into a worm (Waterston, 1989; Barstead and Waterston, 1991; Williams and Waterston, 1994).

Perlecan does not appear to be made by tissues other than muscle during embryonic development. It also does not appear to have a role in muscle cell migration during embryonic development. The terminal phenotype of a null allele of *unc-52* is after muscle quadrants are formed. The primary role of this protein seems to be that of muscle attachment and as an aid to sarcomere organization within a muscle cell (Rogalski *et al.*, 1993, 1995; Williams and Waterston, 1994). The limited distribution of perlecan to the ECM under muscle suggested to us that perlecan may be a cell autonomous product of muscle. Our demonstration that this is indeed the case is to our knowledge the first direct evidence that an ECM component is limited to the region adjacent to the cell of origin. How might this occur? A water-soluble protein can diffuse 10 μm in a second, and a virus particle can diffuse the same distance in 10 sec (cited in Bray, 1992). The gap between muscle cells in the dorsal muscle quadrant caused by the ablation of the D blastomere is between 5 and 10 μm. A soluble protein could clearly traverse this gap and accumulate to detectable levels in the time of our analysis (perlecan would be accumulating in the extracellular environment for at least 1 hr, possibly longer—see above). However, under physiological conditions nematode perlecan is insoluble, which would preclude ready diffusion (Francis and Waterston, 1991). Our results, then, are consistent with what is known about the molecu-

FIG. 7. Nomarski optics micrographs illustrating the range of D-ablated phenotypes. The panels to the left (A, C, E, G, and I) are D-ablated animals at between 390 and 430 min post-first cleavage. The arrows in each of these panels point to the D-ablated material. The panels on the right (B, D, F, H, and J) illustrate examples of a typical developmental pattern followed by each of these ablation types. (A) An embryo with the ablated material segregated as an internal ball. (B) A near-normal L1 larva that developed from the embryo in (A). (C) An embryo with the ablated material excluded from the embryo; and (D) the near-normal L1 larva that developed from this embryo. (E) An embryo similar to (A), but in this case the hatched larva (F) has an indentation where the D-derived muscles should normally be placed (identified by the arrows). (G) An embryo with an excluded ball, as in (C), but in this case the animal developed to a larva with several severe constrictions (H, arrow identifies constriction). (I) We show an example of an embryo with an exluded ball of ablated material (long arrow) that is still attached to the main body of the embryo (short arrow). This animal developed into the ''monster'' shown in (J) sometime within the next 2 hr. The animals shown in (H) and (J) represent terminal phenotypes, while animals exhibiting the (B), (D), or (F) phenotypes usually developed much further (see Table 2). Bar, 10 μm.

lar properties of this protein. Local limited distribution of a major component of the ECM can be viewed as a form of regulation. This limitation is probably essential during development since the ECM has instructional as well as structural roles (Adams and Watt, 1993; Hay, 1991). For example, modulating the ''stickiness'' of cells is an important aspect in such processes as cell–cell contact and cell migration. A freely diffusible ''glue'' would destroy the specificity of such interactions.

A new feature of muscle behavior during *C. elegans* morphogenesis has emerged from our study of the ECM and cell autonomy. We refer to this as plasticity of cell shape. Earlier studies had demonstrated that laser ablation of muscle precursors led to larvae lacking the requisite number of cells (Sulston *et al.*, 1983). Our experiment to examine the cell autonomous behavior of perlecan was based on these observations. We were therefore surprised to observe several embryos with no apparent gap in the appropriate muscle quadrant after laser ablation of a precursor to a patch of muscle cells in this quadrant (Table 1). It has been suggested that muscle cells adjacent to a gap possibly lack the ability to alter their cell length or that they lack surface adhesion molecules necessary to bridge the gap (Hedgecock *et al.*, 1987), but we show here that muscle cells clearly have the ability to compensate for missing components by altering their length and shape. This plasticity of form has permitted the development of a continuous muscle quadrant in animals lacking as many as 6 muscle cells from a quadrant of 21 cells. Sulston and White (1980) have observed a similar phenomenon postembryonically; both hypodermal and intestinal cells can grow to replace missing neighbors. Postembryonic mesodermal tissue also exhibits functional regulation. The response of muscle cells in the male tail to ablation of neighboring muscle cells suggests that there may be competition for specific attachment sites (Sulston and White, 1980).

Perhaps the gap repair we observe in embryos with fewer muscle cells is a variation on this theme. Throughout the time period when muscle cells are migrating from the midline to form the four muscle quadrants, a series of related changes are occurring in the hypodermis which will eventually culminate in muscle–hypodermal attachment. Gradually from approx. 290 min onward intermediate filaments of the hypodermis become apparent and by 430–450 min these have organized into hemidesmosomes, the hypodermal attachment sites for muscle (Hresko *et al.*, 1994; Francis and Waterston, 1991; Goh and Bogaert, 1991). At 310 min these presumptive hypodermal attachment structures have already started to concentrate under muscle cells and by 390 min they are concentrated under the muscle contractile complex (Hresko *et al.*, 1994; Goh and Bogaert, 1991). The recruitment of a hemidesmosomal complex within the hypodermis appears to be the result of a signal received from the underlying muscle. It has been shown that hypodermal cells organize hemidesmosomes only in regions adjacent to muscle cells and not in regions adjacent to areas missing muscle cells (P. Shrimankar and R. H. Waterston, cited in Hresko *et al.*, 1994). Therefore, we presume that potential attachment sites along the hypodermis only become available to muscle cells adjacent to a gap after these cells have invaded the gap and made contact with the underlying hypodermis in this region. This signaling may have to occur during muscle cell migration for an attachment between muscle and hypodermis to occur in this region. This migration period would also be the most opportune time for muscle cell–cell contacts within the gap region to occur. As shown in Fig. 6C, processes between muscle cells could stretch over a long interval once in contact.

Gap repair of dorsal muscle quadrants appears to be a stochastic process. This is not the case for the ventral quadrants, where the gaps are always repaired. A major difference between these two regions is the size of the gap (see Fig. 1D). If, as postulated above, cell–cell contacts are necessary to bridge a gap, these would be much more likely to occur in regions with smaller gaps. Perhaps the limited window of opportunity during migration into the dorsal quadrants does not always allow enough time for the changes in muscle cell shape and mobility that are necessary to bridge a larger gap to occur. As well, gap size will continue to grow as the animal elongates, which will make gap repair even less likely as development proceeds. Note that it is only in the latter phase of this dynamic process that we detect perlecan accumulation in the ECM; i.e., only after migration and shape changes does the cell secrete the components for attachment. In fact, once attachment has occurred, it might inhibit any further gap filling.

Junkersdorf and Schierenberg (1992) have also reported that D-ablated embryos can hatch and develop into fertile adults. Their observations in addition to our studies point out that the D blastomere is clearly not essential for viability in the strictest sense, but without this blastomere one does not observe a wildtype animal in most situations. An unexpected finding from this study was the effect on fecundity observed in several of the ablated animals (Table 2). The effect may be due to damage to the blastomere P4, the germline precursor, during laser irradiation. This blastomere is adjacent to D (see Figs. 1A and 1B). Examination of the data in Table 2 suggests this might not be the complete explanation for the variable brood sizes. Invariably, the more mobile animals have the highest brood sizes, which suggests that brood size simply reflects the overall health of an animal. Presumably the healthiest animals were those that best compensated for the missing muscle cells.

Our results have implications in regard to developmental genetic studies of *C. elegans* muscle. One can view laser-ablated animals as phenocopies of what one might expect to observe in animals with a mutation affecting a subset of the body wall muscle cells. Indeed, the animals shown in Figs. 7F and 7H are strikingly similar to animals lacking or mosaic for CeMyoD (Chen *et al.*, 1994; Krause, 1995). Two broad phenotypic classes of lethal mutants affecting early muscle have been described in *C. elegans*, the Mup class

(muscle positioning; Hedgecock *et al.*, 1987; Goh and Bogaert, 1991) and the Pat class (paralyzed and arrested elongation at twofold; Williams and Waterston, 1994). These mutants are primarily embryonic or early larval lethals. For some of these mutants the gene and its product are known, and these are either components of the attachment complex (e.g., vinculin, Barstead and Waterston, 1991; beta-integrin, Gettner *et al.*, 1995; perlecan, Rogalski *et al.*, 1993) or essential components within the sarcomere (e.g., the minor body wall myosin heavy chain, mhcA, Waterston, 1989). In these examples, all of the body wall muscle cells are affected, which leaves no opportunity for the type of regulation described here to come into play. Mutations affecting only a subset of muscle cells may display a ''leaky'' phenotype, a result of muscle plasticity. Perhaps one needs to cast a wider net when looking for mutations affecting early muscle development.

Plasticity of form in the embryo leads to an interesting situation when the loss of the entire contingent of cells from a blastomere can still yield a viable fertile animal similar to a wildtype animal. Have we inadvertently uncovered a form of functional redundancy within the developing embryo? Certainly form plasticity offers a buffer against the loss of single cells within a structure made of like, or similar, cells. From an evolutionary perspective, shape plasticity might be the means to make new structures rapidly, perhaps occasionally eliminating the long period of tinkering generally believed necessary to make new adaptive structures. Interestingly, the major examples of this regulation of shape in *C. elegans* occur in tissues which display dramatic increases in cell size during postembryonic development: the hypodermis, the intestine, and muscle (Sulston and White, 1980; Sulston *et al.*, 1983, our results). Form plasticity may simply be a manifestation of the endogenous growth program. In *C. elegans* there is a 10-fold increase in length from an L1 larva to a mature adult worm, but body wall muscle cell number only increases from 81 to 95 cells (Sulston and Horvitz, 1977). Individual cell growth is therefore an important parameter for increasing animal size in this organism. Other species may have adopted a compromise strategy to attain larger size, since species with many more than 95 body wall muscle cells have been described (Rosenbluth, 1965).

ACKNOWLEDGMENTS

We thank John Sulston and Einhard Schierenberg for their interest and helpful comments pertaining to D ablations and J.S. for pointing out the possible parallel between our observations and his earlier study on spicule retractor muscles. We thank Ross Francis, Michelle Hresko, and P. Shrimankar for permission to cite their unpublished results. We also thank several colleagues for their comments and suggestions, including Heinke Schnabel, Richard Feichtinger, Bob Barstead, Thierry Bogaert, Martin Adamson, Rupert Timpl, and Bob Waterston. We thank the following for providing antibodies: David Miller and Henry Epstein for mAb DM5.6, Ross Francis for MH2/3 and MH27, and Thierry Bogaert for NE8 4C6.3. Part of this study was supported by a grant from the Deutsche Forschungsgemeinschaft to R.S. D.G.M. gratefully acknowledges the support of a Killam Research Fellowship and also thanks the Max-Planck Society for their support and hospitality. Part of this study was also supported by grants from the Medical Research Council of Canada and the Natural Sciences and Engineering Research Council of Canada to D.G.M.

REFERENCES

Adams, J. C. and Watt, F. M. (1993). Regulation of development and differentiation by the extracellular matrix. *Development* **117,** 1183–1198.

Barstead, R. J., and Waterston, R. H. (1991). Vinculin is essential for muscle function in the nematode. *J. Cell Biol.* **114**(4), 715–724.

Bray, D. (1992). ''Cell Movements.'' Garland, New York, London.

Brenner, S. (1974). The genetics of *Caenorhabditis elegans. Genetics* **77,** 71–94.

Chen, L., Krause, M., Sepanski, M. and Fire, A. (1994). The *Caenorhabditis elegans* MYOD homologue HLH-1 is essential for proper muscle function and complete morphogenesis. *Development* **120,** 1631–1641.

Epstein, H. F., Casey, D. L., and Ortiz, I. (1993). Myosin and paramyosin of *Caenorhabditis elegans* embryos assemble into nascent structures distinct from thick filaments and multi-filament assemblages. *J. Cell Biol.* **122,** 845–858.

Francis, G. R., and Waterston, R. H. (1985). Muscle organization in *C. elegans:* Localisation of proteins implicated in thin filament attachment and I-band organisation. *J. Cell Biol.* **101,** 1532–1549.

Francis, G. R., and Waterston, R. H. (1991). Muscle cell attachment in *Caenorhabditis elegans. J. Cell Biol.* **114**(3), 465–479.

Gettner, S. N., Kenyon, C., and Reichardt, L. F. (1995). Characterization of beta-pat-3 heterodimers, a family of essential integrin receptors in *C. elegans. J. Cell Biol.* **129,** 1127–1141.

Goh, P., and Bogaert, T. (1991). Positioning and maintenance of embryonic body wall muscle attachments in *C. elegans* requires the mup-1 gene. *Development* **111,** 667–681.

Guo, X., Johnson, J. J., and Kramer, J. M. (1991). Embryonic lethality caused by mutations in basement membrane collagen of *C. elegans. Nature* **349,** 707–709.

Hay, E. D. (1991). Collagen and other matrix proteins in embryogenesis. *In* ''Cell Biology of the Extracellular Matrix,'' pp. 419–462. Plenum, New York.

Hedgecock, E. M., Culotti, J. G., Hall, D. H., and Stern, B. D. (1987). Genetics of cell and axon migrations in *Caenorhabditis elegans. Development* **100,** 365–382.

Hird, S., and White, J. G. (1993). Cortical and cytoplasmic flow polarity in early embryonic cells of *Caenorhabditis elegans. J. Cell Biol.* **121**(6), 1343–1355.

Hresko, M. C., Williams, B. D., and Waterston, R. H. (1994). Assembly of body wall muscle and muscle cell attachment structures in *Caenorhabditis elegans. J. Cell Biol.* **124**(4), 491–506.

Hutter, H., and Schnabel, R. (1994). glp-1 and inductions establishing embryonic axes in *C. elegans. Development* **120,** 2051–2064.

Junkersdorf, B., and Schierenberg, E. (1992). Embryogenesis in *C. elegans* after elimination of individual blastomeres or induced

alteration of the cell division order. *Roux's Arch. Dev. Biol.* **202,** 17–22.

Kramer, J. M. (1994). Genetic analysis of extracellular matrix in *C. elegans. Annu. Rev. Genetics* **28,** 95–116.

Krause, M. (1995). MyoD and myogenesis in *C. elegans. BioEssays* **17**(3), 219–227.

MacKenzie, J. M., Garcea, R. L., Zengel, J. M., and Epstein, H. F. (1978). Muscle development in *Caenorhabditis elegans:* Mutants exhibiting retarded sarcomere development. *Cell* **15,** 751–762.

Miller, D. M., Ortiz, G. C., Berliner, G. C., and Epstein, H. F. (1983). Differential localization of two myosins within nematode thick filaments. *Cell* **34,** 477–490.

Podbilewicz, B., and White, J. G. (1994). Cell fusions in the developing epithelia of *C. elegans. Dev. Biol.* **161,** 408–424.

Priess, J. R., and Hirsh, D. I. (1986). *Caenorhabditis elegans* morphogenesis: The role of the cytoskeleton in elongation of the embryo. *Dev. Biol.* **117,** 156–173.

Rogalski, T. M., Williams, B. D., Mullen, G. P., and Moerman, D. G. (1993). Products of the *unc-52* gene in *Caenorhabditis elegans* are homologous to the core protein of the mammalian basement membrane heparan sulfate proteoglycan. *Genes Dev.* **7,** 1471–1484.

Rogalski, T. M., Gilchrist, E. J., Mullen, G. P., and Moerman, D. G. (1995). Mutations in the *unc-52* gene responsible for body wall muscle defects in adult *Caenorhabditis elegans* are located in alternatively spliced exons. *Genetics* **139,** 159–169.

Rosenbluth, J. (1965). Structural organization of obliquely striated muscle fibers in *Ascaris lumbricoides. J. Cell. Biol.* **25,** 495–515.

Schwarzbauer, J. E., and Spencer, C. S. (1993). The *Caenorhabditis elegans* homologue of the extracellular calcium binding protein SPARC/osteonectin affects nematode body morphology and mobility. *Mol. Biol. Cell* **4,** 941–952.

Sibley, M. H., Johnson, J. J., Mello, C. C., and Kramer, J. M. (1993). Genetic identification, sequence, and alternative splicing of the *Caenorhabditis elegans* alpha(IV) collagen gene. *J. Cell Biol.* **123**(1), 255–264.

Sibley, M. H., Graham, P. L., von Mende, N., and Kramer, J. M. (1994). Mutations in the alpha2(IV) basement membrane collagen gene of *Caenorhabditis elegans* produce phenotypes of differing severities. *EMBO J.* **13**(14), 3278–3285.

Smith, D. B., and Johnson, K. S. (1988). Single-step purification of polypeptides expressed in *Escherichia coli* as fusions with glutathione *S*-transferase. *Gene* **67,** 31–40.

Sulston, J. E., and Horvitz, H. R. (1977). Postembyonic cell lineages of the nematode *Caenorhabditis elegans. Dev. Biol.* **82,** 41–55.

Sulston, J. E., and White, J. G. (1980). Regulation and cell autonomy during postembryonic development of *Caenorhabditis elegans. Dev. Biol.* **78,** 577–597.

Sulston, J. E., Schierenberg, E., White, J. G., and Thomson, J. N. (1983). The embryonic cell lineage of the nematode *Caenorhabditis elegans. Dev. Biol.* **100,** 64–119.

Towbin, H., Staehelin, T., and Gordon, J. (1979). Electrophoretic transfer of proteins from polyacrylamide gels to nitrocellulose sheets: Procedure and some applications. *Proc. Natl. Acad. Sci. USA* **76,** 4350–4354.

Waterston, R. H., Thomson, J. N., and Brenner, S. (1980). Mutants with altered muscle structure in *Caenorhabditis elegans. Dev. Biol.* **77,** 271–302.

Waterston, R. H. (1988). Muscle. *In* ''The Nematode *Caenorhabditis elegans*'' (W. B. Wood, Ed.), pp. 281–335. Cold Spring Harbor Laboratory, Cold Spring Harbor, NY.

Waterston, R. H. (1989). The minor myosin heavy chain, MHC A, of *Caenorhabditis elegans* is necessary for the initiation of thick filament assembly. *EMBO J.* **8,** 3429–3436.

White, J. G., Southgate, E., Thomson, J. N., and Brenner, S. (1986). The structure of the nervous system of the nematode *Caenorhabditis elegans. Phil. Trans. R. Soc. B* **314,** 1–340.

White, J. (1988). The Anatomy. *In* ''The Nematode *Caenorhabditis elegans*'' (W.B. Wood, Ed.), pp. 81–122. Cold Spring Harbor Laboratory, Cold Spring Harbor, NY.

Williams, B., and Waterston, R. H. (1994). Genes critical for muscle development and function in *Caenorhabditis elegans* identified through lethal mutations. *J. Cell Biol.* **124**(4), 475–490.

Received for publication July 5, 1995
Accepted September 29, 1995